



# Room temperature hardness of carbides-strengthened cast alloys in relation with their carbon content and the aging temperature. Part II: Case of cobalt alloys

Patrice Berthod

## ► To cite this version:

Patrice Berthod. Room temperature hardness of carbides-strengthened cast alloys in relation with their carbon content and the aging temperature. Part II: Case of cobalt alloys. Materials Science and Technology, 2009, pp.663 - 669. 10.1179/174328408X339251 . hal-02431616

**HAL Id: hal-02431616**

**<https://hal.science/hal-02431616>**

Submitted on 8 Jan 2020

**HAL** is a multi-disciplinary open access archive for the deposit and dissemination of scientific research documents, whether they are published or not. The documents may come from teaching and research institutions in France or abroad, or from public or private research centers.

L'archive ouverte pluridisciplinaire **HAL**, est destinée au dépôt et à la diffusion de documents scientifiques de niveau recherche, publiés ou non, émanant des établissements d'enseignement et de recherche français ou étrangers, des laboratoires publics ou privés.

# **Room temperature hardness of carbides-strengthened cast alloys in relation with their carbon content and the aging temperature.**

## **Part II: Case of cobalt alloys**

Patrice BERTHOD

Laboratoire de Chimie du Solide Minéral (CNRS UMR 7555)

Faculté des Sciences et Techniques, Université Henri Poincaré Nancy 1, Nancy-Université,

Boulevard des Aiguillettes, BP 239, F-54506 VANDOEUVRE LES NANCY, FRANCE

patrice.berthod@centraliens-lille.org

Post-print version of the article: *Materials Science and Technology* (2009) 25(5) 663-669.

DOI 10.1179/174328408X339251

**Keywords:** Cobalt alloy, Chromium carbides, Tantalum carbides, Aging treatment, Vickers indentation, Macro and microhardness

### **Abstract.**

Nine cobalt alloys, all containing 30wt.%Cr, various carbon contents and two amounts of tantalum (for two of them), were elaborated by casting and aged at 1,000, 1,100 and 1,200°C for 50 hours. The hardness of each sample was measured by macro and micro Vickers indentation, and studied in accordance with the carbon content, the nature and fractions of carbides. The hardness increases from about 250-270 up to 500-550, which is the prolongation of the range for nickel alloys with similar compositions. The increase in hardness with the carbon content obeys a linear function of the carbon content, which allows choosing a carbon content to achieve a targeted hardness, in the studied range of carbon or by extrapolation to higher values. For a same carbide fraction, hardness significantly depends on the nature of carbides (e.g. higher for TaC than for  $M_7C_3$  carbides).

### **1. Introduction**

Cobalt alloyed with chromium is used as a matrix in numerous applications. Like in the first article of this work concerning nickel alloys<sup>1</sup>, one can cite again alloys for prosthetic dentistry<sup>2</sup>, aeronautics and power generation<sup>3</sup> and even glass forming tools<sup>4</sup>. In such fields,

several tens weight percent of chromium are commonly added to cobalt in order to give to the alloy a sufficient resistance against wet or atmospheric corrosion, hot corrosion by molten salts or glass, and high temperature oxidation. For such applications, the question of hardness is already of a great importance since cobalt, which is already a hard element, tends to increase the hardness of alloys, by comparison with nickel or iron-based alloys. This notably leads to enhanced difficulties of machining. Another use of cobalt, in which this high hardness is exploited, is cutting tools, in which cobalt is mixed with harder particles to form Co-WC materials<sup>5</sup> or coatings as Co-W<sub>2</sub>C thermal sprayed on steels<sup>6</sup>.

This second part of this study is an exploration of the range of the possible hardness that nickel-free cast cobalt-base alloys can exhibit with the types of carbides which can appear during their solidification, and which can be stabilized by heat treatments at high temperature. Two types of carbides were of interest: chromium carbides which can be obtained in simple corrosion-resistant ternary alloys (Co-Cr-C) with a wide range of carbon contents, and tantalum carbides in quaternary corrosion-resistant Co-Cr-C-Ta alloys, for medium carbon contents.

## 2. Experimental

The experimental details of this second part of this work were, for most of them, already presented in the first article<sup>1</sup>. These can be summarized as follows.

The seven alloys are all {Co-30wt.%Cr}-based and contain the same carbon contents that the nickel alloys of the first part of this study, i.e. 0, 0.2, 0.4, 0.8, 1.2, 1.6 and 2.0 wt.%C, and they are named following the same system (from Co00 to Co20). They were induction melted and cast under Argon from pure elements (cobalt and chromium: Alfa Aesar, purity > 99.9wt.%; carbon: graphite). In each case three ( $10 \times 10 \times 3 \text{ mm}^3$ ) samples, polished with 1,200 grit paper, underwent a 50h exposure at 1,000°C, 1,100°C or 1,200°C, followed with a  $10 \text{ K min}^{-1}$  cooling. They were cut, embedded and mirror-like polished, then etched with the Groesbeck solution to obtain mounted samples for metallographic observations using optical microscope, identification of carbides by Wavelength Dispersion Spectrometry, measurement of carbide fractions by image analysis, and Vickers hardness (load = 30kg) + microhardness (load = 8g, only for matrixes) measurements.

Thermodynamic calculations were also performed to complete the knowledge of the phases present at high or lower temperatures, using the Thermo-Calc software<sup>7</sup> and the database containing the descriptions of the Co-Cr-C system and its sub-systems (SSOL<sup>8</sup>).

Two other alloys were additionally elaborated and studied following the same procedures: these ones are two Ta-containing {Co-30wt.%Cr}-based alloys, the first one with 0.3 wt.%C and 4.2 wt.%Ta, and the second one with 0.8 wt.%C and 7.7 wt.%Ta (EDS analysis with SEM), in order to complete the study by involving a second type of carbide, TaC, for the medium values of carbon content among the six first ones. For these two additional alloys, thermodynamic calculations also used the description of systems involving Ta: Co-Ta, Cr-Ta, C-Ta and Co-C-Ta<sup>9-12</sup>.

### 3. Results

#### 3.1 Microstructures of the Co-30Cr-xC alloys

The microstructures of the ternary alloys are illustrated in Fig. 1 by optical micrographs (taken after Groesbeck etching) for the two extreme temperatures of aging treatment, 1,000°C and 1,200°C, except in the case of the low-carbon alloys for which 1,200°C led to a local or general catastrophic oxidation which induced a partial or total disappearance of carbides in the alloy<sup>13</sup>. Thus, for the latter alloys, only the microstructures after aging at 1,000°C are represented (however etching did not lead to very clear micrographs because of the too small quantities of carbides).

In all cases one can see the dendritic matrix of the alloys (except for the Co00 binary alloy, the microstructure of which was not evidenced by carbides coloration due to etching), and that more easily for the carbide-richest alloys than for the other. Carbides are all interdendritic, and they are obviously of two types. They are  $M_7C_3$  for the carbon-richest alloys since they are clearly coloured in brown by the Groesbeck etching. For the alloys with less carbon, in contrast, they tend to be more  $M_{23}C_6$  because of their grey/pale blue coloration (which is more or less visible since carbides are very small in these alloys). WDS microanalysis measurements, only possible for the carbon-richest alloys (Co20, Co16, Co12 for the three temperatures, and Co08 for 1,100 and 1,200°C), clearly showed that carbides are effectively  $M_7C_3$  in their cases, while the  $M_{23}C_6$  of the other alloys were identified only by coloration. These stoichiometries of carbides, which did not really change during the too short cooling, are also that ones which are predicted by Thermo-Calc for the studied carbon content and temperatures<sup>14</sup>. About the matrixes, if they were in all cases austenitic (FCC) at solidification, they became HCP at medium (less than 950°C) to low temperatures, i.e. at



room temperature. This was also verified by Thermo-Calc calculations and can be experimentally detected by thermodilatometry measurements<sup>15</sup>, for example.

Like for the nickel alloys, carbides are here logically more present in the alloy when the carbon content of the latter is high. Their morphology obviously depends on the aging temperature (more compact or rounder for 1,200°C than for 1,100 and 1,000°C). Surface fractions of carbides were quantified by image analysis, what was possible since the contrast between dark carbides and pale matrix obtained after Groesbeck etching was sufficient. Fig. 2 graphically presents the results (average value for three micrographs  $\pm$  standard deviation), which are, here too, consistent with the volume fractions deduced by conversion of the mass fractions calculated with Thermo-Calc. The surface fraction increases almost linearly when the carbon content in the alloy increases (and also slightly decreases when the aging temperature increases). This linearity exists here up to the maximum carbon content (2 wt.%), unlike the nickel alloys for which the increase was lowered for the highest carbon contents. In contrast, like for the similar nickel alloys of the first part of this study, the rate is, here too, of about 12 surface percent per carbon weight percent, and the surface fraction of carbides tends to be slightly lower when the aging temperature was higher.

### 3.2 Vickers macro-hardness and micro-hardness of the Co-30Cr-xC alloys

The Vickers hardness values (load of 30kg) near the middle of each sample are plotted in the two graphs of Fig. 3 (average value of three measures and standard deviation as uncertainty), for all alloys aged at 1,000°C and 1,100°C. For 1,200°C, only the three carbon-richest alloys were considered since the other partly or totally lost their carbides because of oxidation. Like for nickel alloys, one can see the increase in hardness when the carbon content increases (left hand graph), which is quite linear. One finds again, for a given carbon content, the decrease in hardness when the temperature of the aging treatment increases, with a difference of about 20 to 25 hardness units per each hundred degrees. One can notably see that the curves for 1,000°C, 1,100°C and 1,200°C are more clearly separated from one another than in the case of the nickel alloys. The evolution of hardness with the surface carbide fraction as estimated by image analysis (right hand graph) is linear too, with an increasing rate of about 10 Hv<sub>30kg</sub> per volume percent of carbide, *id est* higher than for the nickel alloys.

The Vickers hardness, measured in the matrix of each alloy for each temperature (load = 8g, five measurements per sample), was plotted in Fig.4 versus the chromium content (left hand graph) or the carbon content (right hand graph) in the matrix, by considering the

contents predicted by Thermo-Calc for each {alloy; aging temperature} couple. Results are dispersed, maybe because of the presence, in some cases, of subjacent primary carbides (and even of secondary carbides for samples treated at 1,000°C). It is then difficult to see any possible dependence of the matrix hardness on the chromium content or on the carbon content. But it is true that the hardness of matrix is generally higher for the carbides-richest alloys, and then it is possible that the above observation results from a limiting effect of the neighbour carbides for the matrix deformation. Then, here too, there is no clear dependence of the hardness of matrix on its chemical composition. However, the average level of hardness of the HCP matrixes of these cobalt-base alloys is significantly higher than the one for the FCC matrixes of the nickel alloys (about 100 - 150 Hv<sub>8g</sub>, higher). Since no of these alloys, which were all obviously hypoeutectic-type, contains a carbide coarse enough to allow performing a Vickers micro-indentation, no hardness of carbide is available in this part of the study. Therefore, the value which was obtained for a very coarse carbide (with the M<sub>7</sub>C<sub>3</sub> stoichiometry too) in the Ni-30Cr-2.0C alloy aged at 1,000°C<sup>1</sup>, was considered for further calculations (1,192 Hv<sub>32g</sub>).

### 3.3 Comparison between the real hardness and a one calculated with a law of mixture

Like for nickel alloys, since the hardness increases linearly with the carbides volume fraction, it was here too attempted to represent the hardness of the whole alloy by a linear combination of the volume fractions of the two phases, multiplied with the separate hardness of matrix and carbides:

$$Hv(\text{all}) = (1 - f_{\text{vol}}(\text{carb})) \times Hv(\text{mat}) + f_{\text{vol}}(\text{carb}) \times Hv(\text{carb})$$

with:

- \* Hv (all) being the average Vickers hardness of the whole alloy (load: 30kg)
- \*  $f_{\text{vol}}(\text{carb})$  equal to the average value of surface fraction measured by image analysis
- \*  $Hv(\text{carb}) = 1,192$  (=Hv<sub>32g</sub> obtained for a coarse M<sub>7</sub>C<sub>3</sub> carbide<sup>1</sup>)
- \* Hv(mat):
  - equal to the average value of the hardness (load 30kg) of the binary alloy Co-30wt.%Cr (curves designed in Fig. 5 by “**theo1**”)
  - or  $Hv(\text{mat}) =$  average value of the micro-hardness (load 8g) of the binary alloy Co-30wt.%Cr (curves designed in Fig. 5 by “**theo2**”)

- or  $H_v(\text{mat})$  = average value of the five micro-hardness (load 8g) values obtained in the matrix of the considered alloy for the considered aging temperature (curves designed in Fig. 5 by “**theo3**”).

The three theoretic curves were superposed in Fig. 5 with the experimental curve (one graph per aging temperature). It is clear that the first theoretic curve (“theo1”, with calculation from the  $H_{v30kg}$  average value of the Co-30wt.%Cr alloy) is closer to the real curve than the two others, and that on the whole carbon range.

### 3.4 Comparison with the two TaC-containing alloys

The microstructures of these alloys are composed of a cobalt solid solution matrix (also FCC at solidification but HCP after cooling down to room temperature), with eutectic tantalum carbides (TaC) and eutectic chromium carbides ( $M_{23}C_6$ ), as revealed by both WDS microanalysis and Thermo-Calc calculations (Fig. 6). The Co-30Cr-0.3C-4.2Ta (contents in wt.%) contains essentially TaC carbides and rare  $M_{23}C_6$  ones (identified by Thermo-Calc only because too small for WDS measurements), while the Co-30Cr-0.8C-7.7Ta contains the two types of carbides with similar volume fractions. When the temperature of the aging treatment increases, the volume fraction of TaC slightly decreases in the two alloys (e.g. 2.2 for 1,000°C and 2.1% for 1,200°C in the case of the 0.3C-4.2Ta alloy), while this decrease is more pronounced for the chromium carbides (e.g. 5.9% for 1,000°C and 4.3% for 1,200°C in the case of the 0.8C-7.7Ta alloy). When applied at a very high temperature, the aging treatment also led to a fragmentation of the TaC script-like carbides, which is particularly visible for the 0.8C-7.7Ta alloy at 1,200°C.

The two alloys present relatively high values of hardness (load 30kg), by comparison to the ternary cobalt alloys with similar carbon contents. It is also true when the volume fractions of carbides are considered. Indeed, the curves of hardness variation versus the total volume fraction (TaC +  $M_{23}C_6$ ) are positioned above the curves corresponding to the Co-30Cr-xC alloys (Fig. 7). Generally, the hardness of the Ta-containing alloys is about 50  $H_{v30kg}$  higher than the Co-30Cr-xC ones for similar carbides fractions.

#### 4. Discussion

For all carbon contents and all aging temperatures the hardness of cobalt alloys is significantly higher than for nickel alloys, what can be related to the difference of the intrinsic hardness of the two matrixes, the FCC one of nickel and the HCP one of cobalt. Like for nickel, adding 30 wt.% of chromium to cobalt did not noticeably change its hardness while, on the contrary, the addition of carbon leads to a significant increase in hardness. For {Co-30 wt.%Cr}-based alloy this increase can be considered as being linear versus the carbon content (about 125Hv<sub>30kg</sub> units per carbon weight percent), as well as versus the volume fraction of carbides (about 10Hv<sub>30kg</sub> units per percent of carbide fraction, i.e. almost twice the slope for nickel alloys). The increase in alloy hardness due to a same increase in carbide fraction is then higher for cobalt alloys than for nickel alloys. This probably results from a more efficient contribution of carbides in the resistance against indentation, since the matrixes of these cobalt alloys, which are harder than the nickel alloys' ones, are less plastically deformed. Then carbides are less displaced and participate more to the resistance against indenter penetration.

The dependence of hardness on the aging treatment is different if the comparison is done for the same carbon content or for a same surface fraction of carbides. Indeed, in the first case, the hardness regularly decreases when the aging treatment temperature increases, while this is more questionable in the second case, especially between 1,000 and 1,100°C. For nickel alloys it was seen that the hardness of low carbon (or low carbides) alloys knows a decrease between 1,000 and 1,100°C (with equals values of hardness between 1,100 and 1,200°C) while this decrease occurs only between 1,100 and 1,200°C for the high carbon or high carbides alloys. Here, for cobalt alloys, the hardness is almost the same for the 1,000°C aging treatment and for the 1,100°C one, for all carbon contents, while the decrease between 1,100 and 1,200°C exists here too for the carbon-richest alloys. Concerning the alloys with the lowest carbon contents, their too low resistance against oxidation at 1,200°C did not allow doing this comparison. The keeping of the hardness between the low-carbon alloys aged at 1,000 and the ones aged at 1,100°C is here probably due to the high intrinsic hardness of the matrix (to compare with nickel alloys) which reduces the dependence of the alloy hardness on the carbides fractions or morphologies. In addition, one can also think that it is the intrinsic hardness of the cobalt-chromium matrix that allows a regular increase in hardness when the carbon content increase. Indeed, the difference of hardness between the Co-(about)30Cr matrix and chromium carbides (generally M<sub>7</sub>C<sub>3</sub>) which is smaller than between the Ni-

(about)30Cr matrix and the same carbides, obviously allows the matrix being not too weak when indentation is performed, and then playing a similar deformation role as carbides. This is probably the reason of the good respect of the law of mixture which was seen here, in addition to a probable role of the dendritic structure which exists for these cobalt alloys from the lowest-carbon alloys to the highest-carbon ones which is maybe also favourable to a good resistance of the matrix to indentation.

The hardness values observed with the TaC-containing alloys are higher than the ones of the  $M_7C_3$ -containing alloys for the same carbides fractions. This can be explained by the values of micro-hardness of TaC carbides and  $M_{23}C_6$  carbides which are about 20% higher than the hardness of  $M_7C_3$  carbides<sup>16</sup>, since the 8g-Vickers micro-hardness values obtained for their matrixes (average value = 325) are similar to the matrix of the ternary Co-30Cr-xC alloys with the same carbon contents. If it can be supposed that the same law of mixture is respected for these TaC-containing alloys too, a possible value of the hardness of carbides (TaC and  $M_{23}C_6$ ) can be deduced from the slope of the straight line representing the average value of the hardness of alloy versus the carbides fraction, (i.e.  $H_v(\text{carb})-H_v(\text{mat})$  with  $H_v(\text{mat}) \cong 325$ ). The deduced value,  $909+325=1234$  is slightly higher (+3%) than the hardness measured in the coarse  $M_7C_3$  carbide ( $H_{v8g}=1192$ ). This value becomes  $1091+325=1416$  if the point corresponding to Co30Cr0.8C7.7Ta aged at 1,000°C is removed, which corresponds to a relative increase of +19%, i.e. the relative increase in hardness from the  $M_7C_3$  to the TaC or  $M_{23}C_6$  carbides<sup>16</sup> (+20%).

## 5. Conclusion

For a same chromium content of 30wt.%, the cobalt alloys display a hardness which is about 200 units of Vickers hardness higher than the nickel alloys with similar carbon contents, a difference which moreover increases with the carbide fraction (from about 150 to 250, for carbon from 0 to 2wt.%). Together the binary and ternary (Ni or Co)-30wt.%Cr-(0 to 2wt.%)C alloys allow achieving hardness from 110 up to 550, the low hardness - part of this range being represented by nickel alloys and the high hardness - part by cobalt alloys. Higher values of hardness can be predicted from the law of mixture (for cobalt alloys only), i.e. about  $H_{v30kg} = 650$  for 3 wt.%C (aging temperature of 1,000°C), a law of mixture which also can be used to adjust the hardness at a targeted value, by deducing the carbon content to choose for the alloy.

Thus, together these nickel alloys and cobalt alloys offer a relatively wide range of hardness (and then probably of wear resistance), adjustable coarsely by the carbon content and the type of carbide, and finely by the aging temperature. The machining easiness of carbides-strengthened nickel-based or cobalt-based alloys and superalloys can also be partially predicted by considering these values, but the type of the carbides are of a significant importance and must be taken into account.

To finish, it can be remembered that a very simple law of mixture can, in some cases, correctly represent the dependence of hardness on the carbide fraction, but it may be also not sufficient in other cases (e.g. other type of matrix). For a better prediction and a wider field of studied alloys, the behaviour of matrixes especially ductile, and also the grain size which can vary following the conditions of alloy elaboration, must be taken into account. The law of mixture used in this study can be a base for building a more general model, integrating matrix hardening during indentation and relationships issued from the Hall-Petch law, for example.

## Aknowledgements

The author gratefully thanks Pierric LEMOINE who elaborated and heat-treated some of the studied alloys.

## References

- [1] P. Berthod: submitted to *Mater. Ci. Technol.*
- [2] D.A. Bridgeport, W.A. Brandtley and P.F. Herman: *Journal of Prosthodontics*, 1993, **2**, 144-150.
- [3] C.T. Sims and W.C. Hagel: 'The superalloys'; 1972, New York, John Wiley & Sons.
- [4] P.Berthod, J.L.Bernard, C.Liébaut: Patent WO99/16919.
- [5] B. Roebuck and E.A. Almond: *Int. Mater. Rev.*, 1988, **33**, 90-110.
- [6] A. Klimpel, L.A. Dobrzanski, A. Lisiecki and D. Janicki: *J. Mater. Process. Tech.*, 2005, **164-165**, 1068-1073.
- [7] Thermo-Calc version N: "Foundation for Computational Thermodynamics" Stockholm, Sweden, Copyright (1993, 2000).
- [8] SGTE: Scientific Group Thermodata Europe database, update 1992.
- [9] Z.K. Liu and Y. Austin Chang: *Calphad*, 1999, **18**, 339-356.
- [10] N. Dupin and I. Ansara: *J. Phase Equilib.*, 1993, **14**, 451-456.

- [11] K. Frisk and A. Fernandez Guillermet: *J. Alloy Compd*, 1996, **238**, 167-179.
- [12] L. Dimitrescu, M. Ekroth and B. Janson: *Metall. Mater. Trans. A*, 2001, **32**, 2167-2174.
- [13] P. Berthod: *Ann. Chim.-Sci. Mater.*, 2008, **6**, in press.
- [14 ] P. Berthod, P. Lemoine and J. Ravaux: *J. Alloy Compd*, 2008, in press.
- [15] P. Berthod: *Int. J. Mat. Res. (formerly Z. Metallkd.)*, 2008, **99**, 265-272.
- [16] G.V. Samsonov: 'High-Temperature. Materials Properties Index'; 1964, New York, Plenum Press.

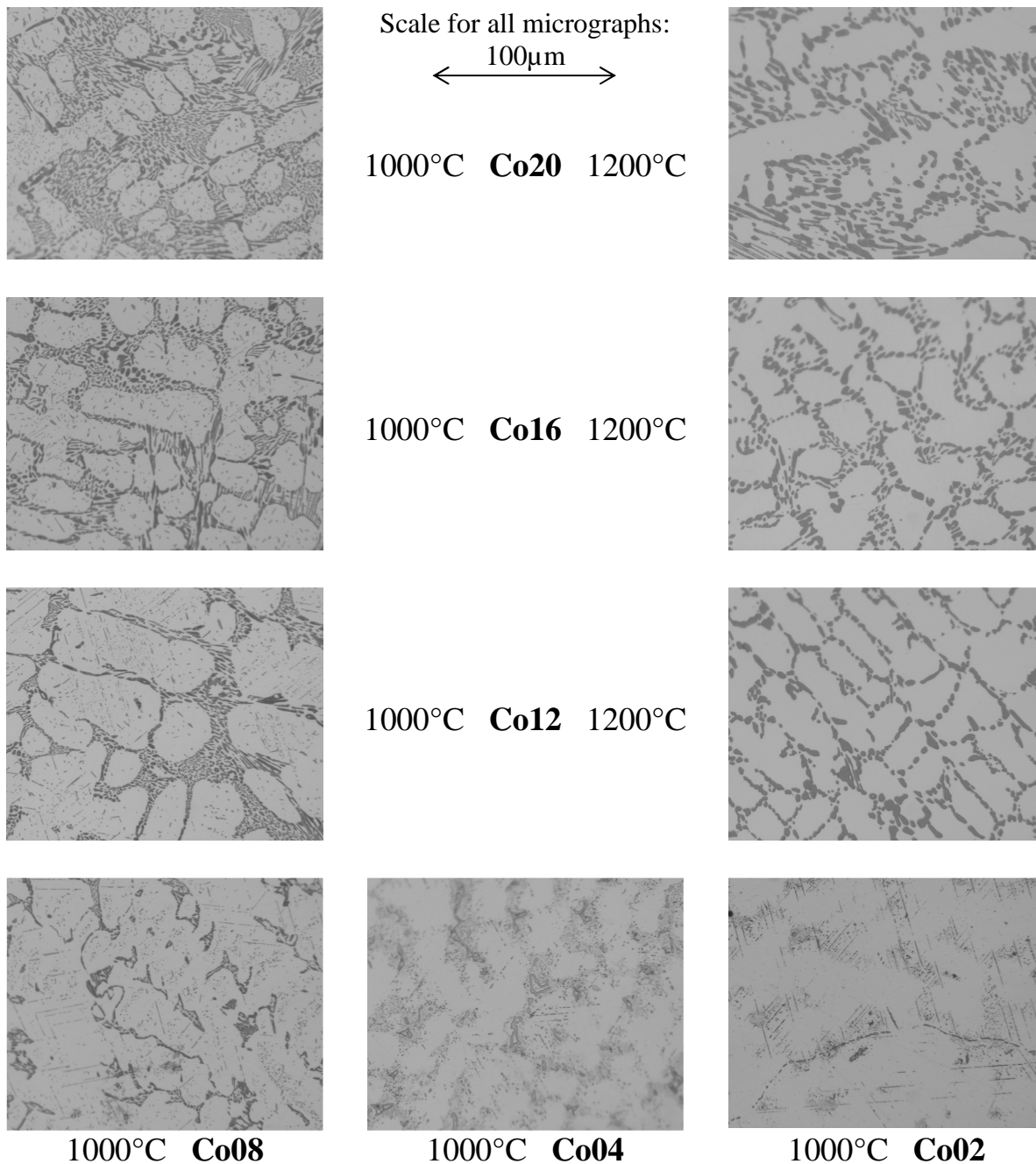


**Fig. 1** Microstructures of the six Co-base C-containing alloys after 50 hours spent at the two extreme temperatures



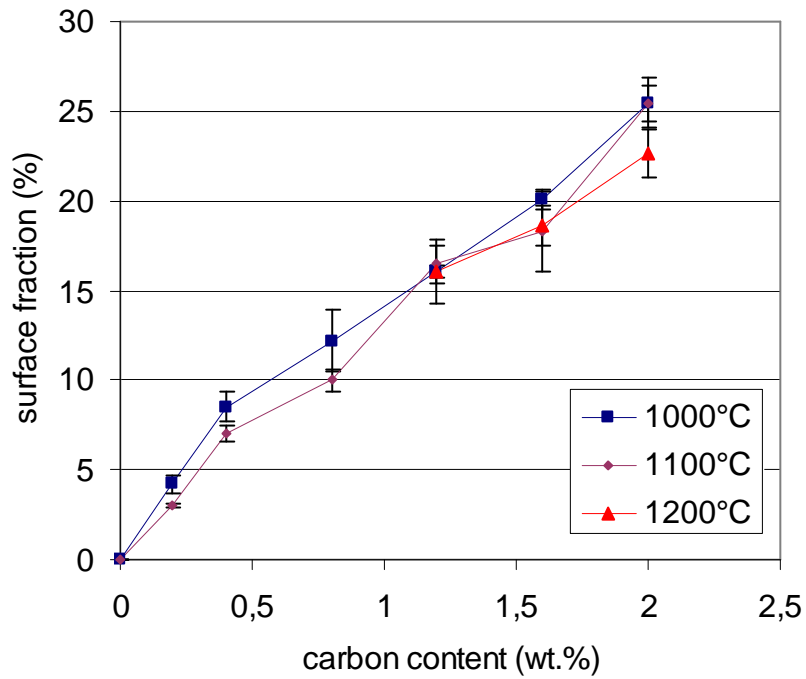


**Fig. 2** Carbides surface fractions of all ternary alloys plotted versus their carbon content for the three aging temperatures; determination by image analysis on three optical micrographs after Groesbeck etching (average value  $\pm$  standard deviation)

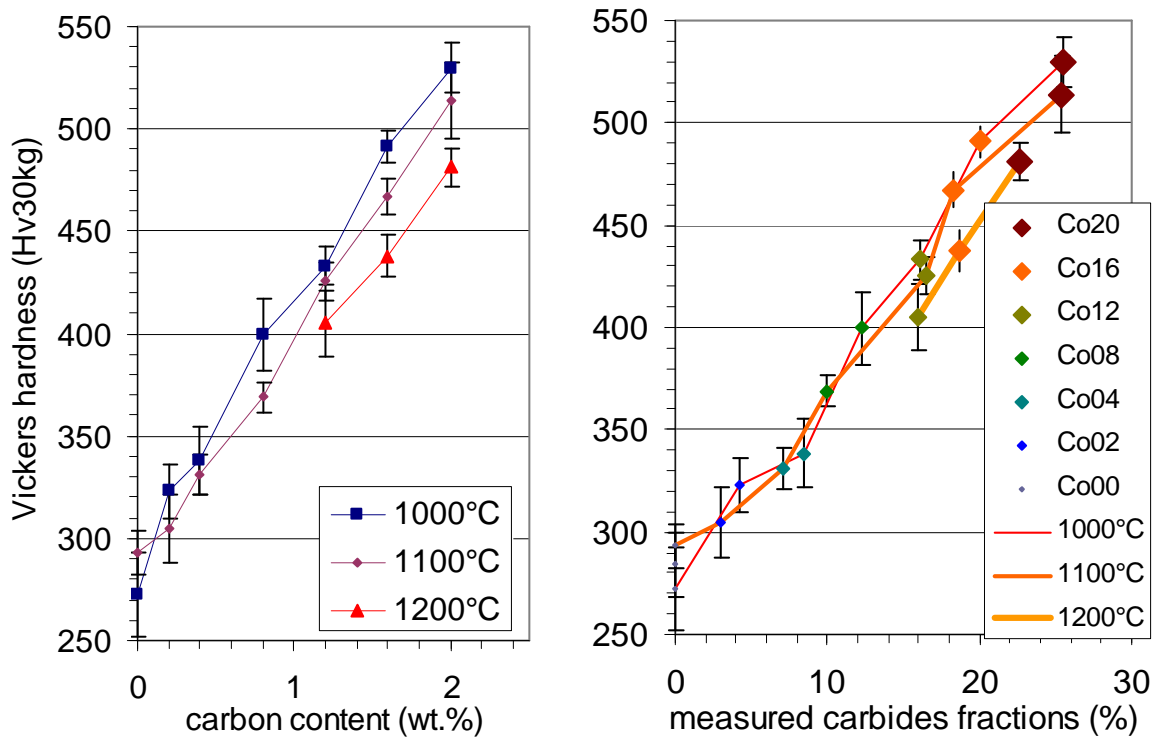


**Fig. 3** Vickers hardness (30kg) of all ternary alloys plotted versus their carbon content (on the left) and versus their carbide fractions (on the right) for the three aging temperatures (average value  $\pm$  standard deviation)

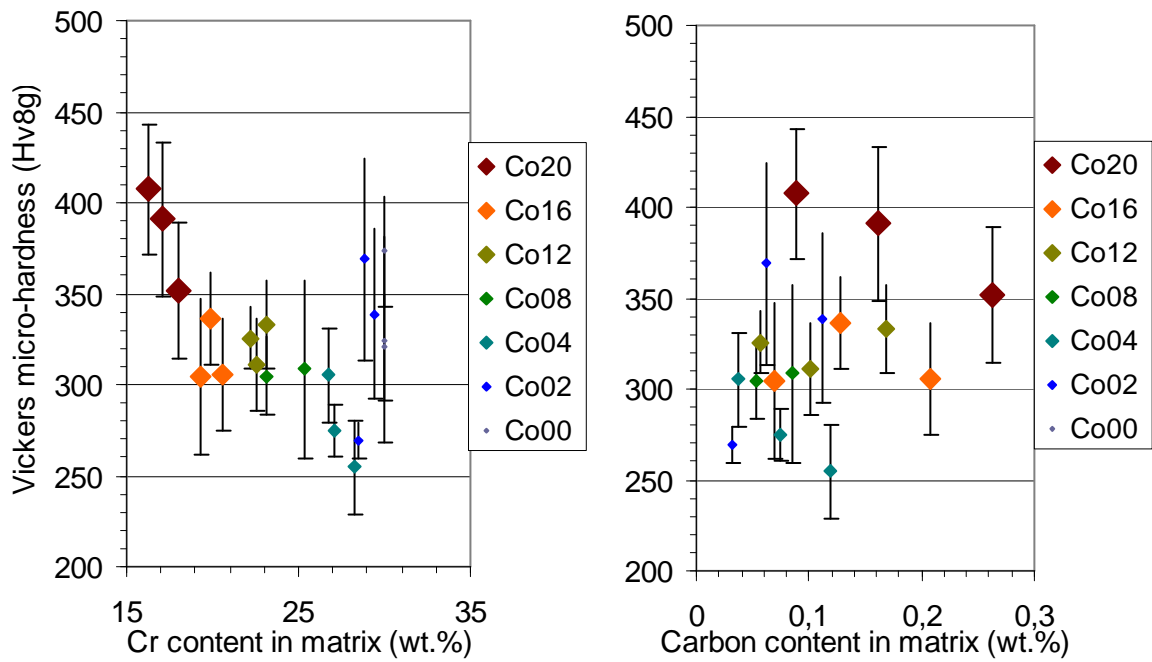


**Fig. 4** Vickers micro-hardness (8 g) of all ternary alloys' matrix plotted versus their chromium content (on the left) and versus their carbon content (on the right) for the three aging temperatures  
(average value  $\pm$  standard deviation)

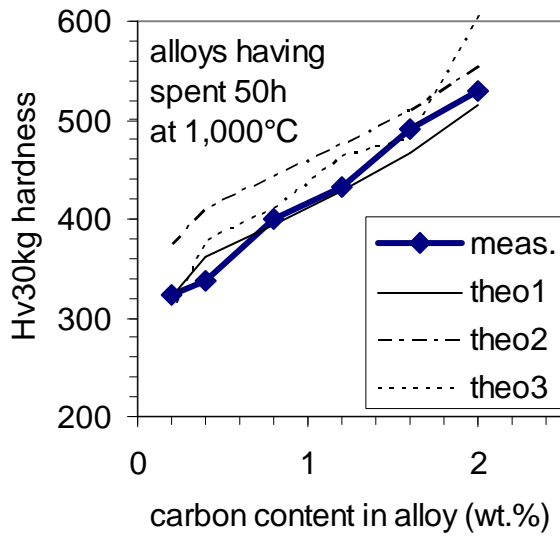
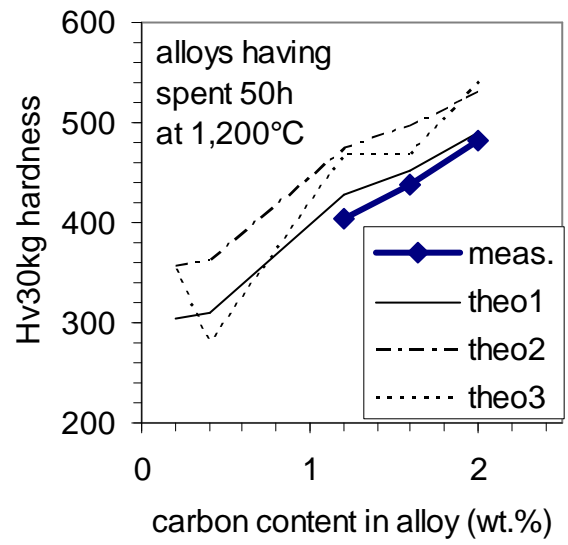
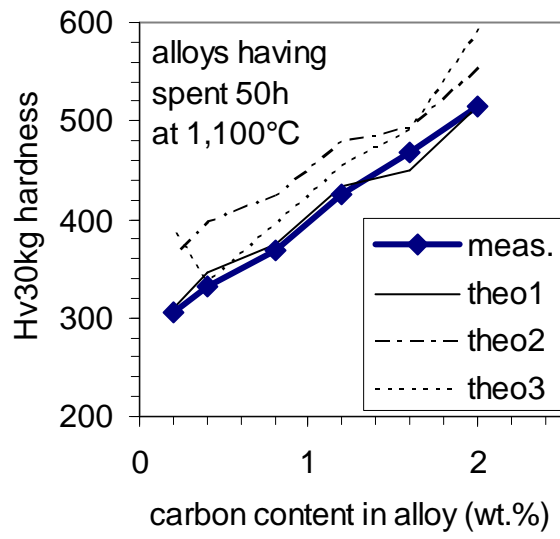


**Fig. 5**

Comparison of the measured hardness of all ternary alloys for all temperatures with the three types of theoretic hardness calculated from the hardness of matrix and the hardness of carbides

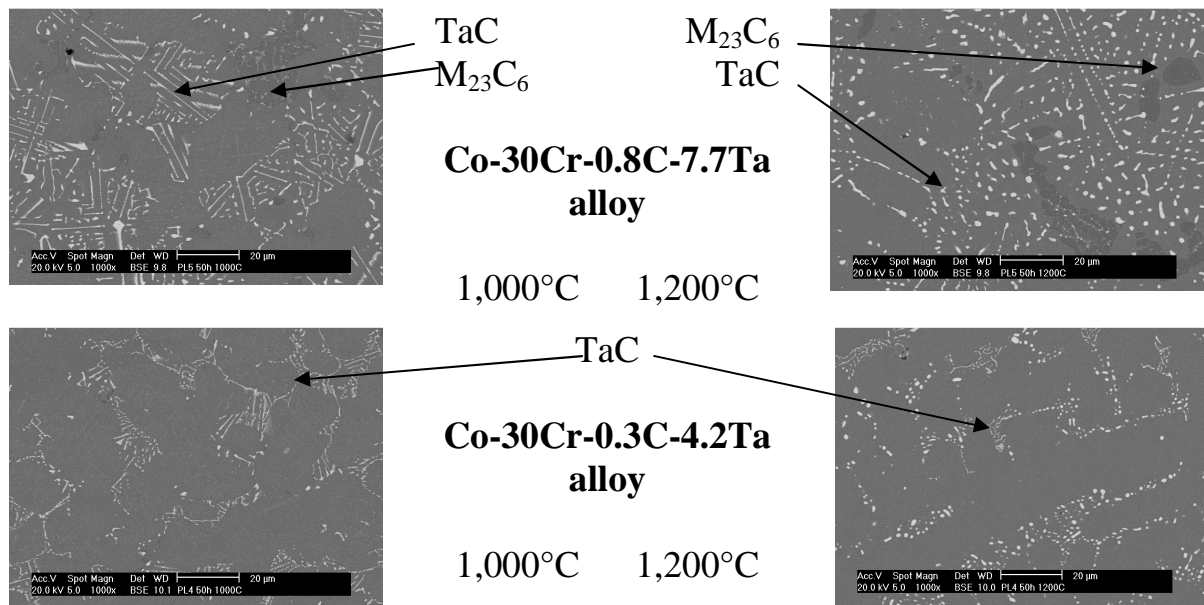


**Fig. 6** Micrographs illustrating the microstructures of the two Ta-containing cobalt alloys after aging at 1,000°C and 1,200°C (SEM in BSE mode)

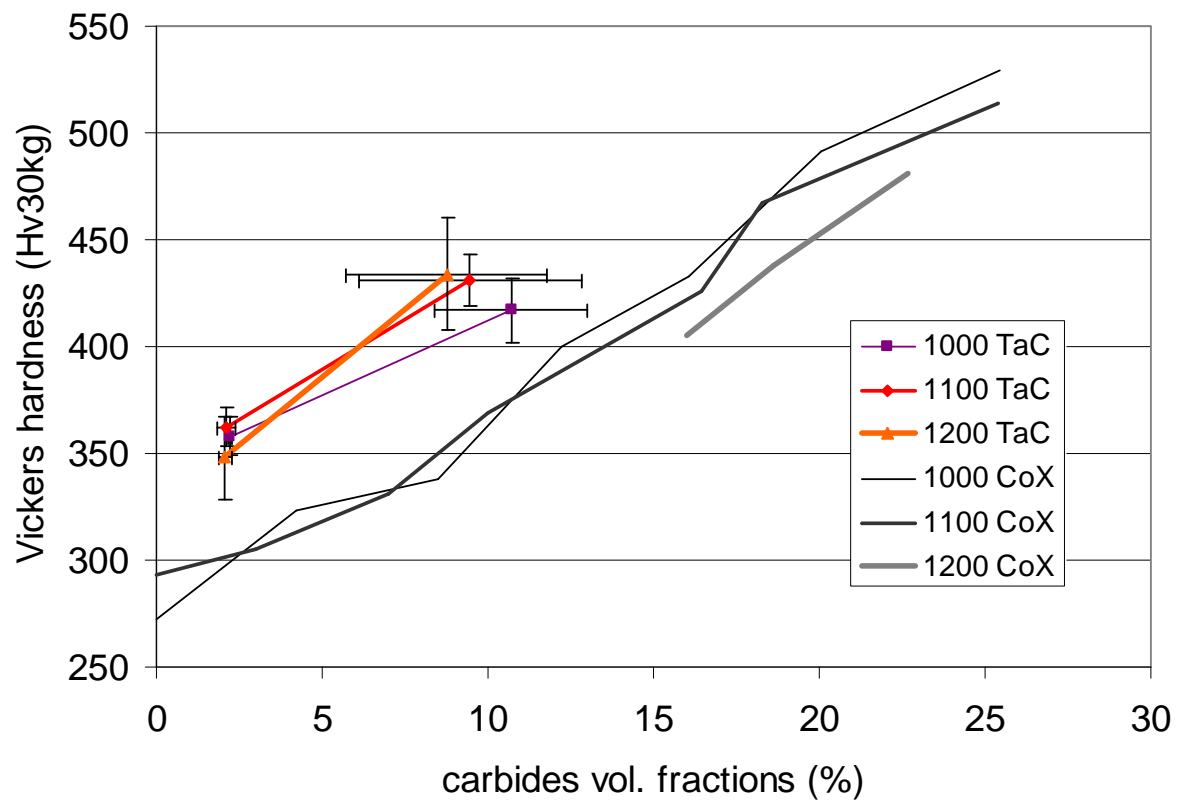


**Fig. 7** Comparison between the hardness of TaC-containing cobalt alloys and  $M_7C_3$ -containing cobalt alloys, for similar volume fractions of carbides